

Cite this: *J. Mater. Chem.*, 2011, **21**, 6769

www.rsc.org/materials

HIGHLIGHT

Hierarchically structured photoelectrodes for dye-sensitized solar cells

Qifeng Zhang and Guozhong Cao*

DOI: 10.1039/c0jm04345a

This paper highlights several significant achievements in dye-sensitized solar cells using hierarchically structured photoelectrodes that consist of spherical or one-dimensional assemblies of ZnO or TiO₂ nanocrystallites. It shows that, besides providing a large surface area for dye adsorption, more importantly, the hierarchically structured photoelectrodes may improve the solar cell's performance by imparting extra functions, such as (1) generating light scattering owing to the size of assemblies being comparable to the wavelengths of the incident light, (2) enhancing electron transport due to the compact packing of the nanocrystallites that form the assemblies, and (3) facilitating electrolyte diffusion as a result of the relatively open structure of the photoelectrode films composed of spherical or one-dimensional assemblies.

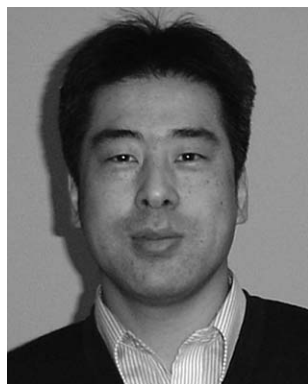
Introduction

Dye-sensitized solar cells (DSCs) are a category of photovoltaic device based on a photoelectrochemical system in which a porous oxide film with dye molecules adsorbed on the surface serves

as the working electrode for light harvesting and the generation of photoexcited electrons.^{1,2} The photogenerated electrons transfer from the dye molecules to the oxide, followed by diffusion in the oxide film and finally they reach a transparent film that conducts the electrons to an external circuit. The oxidized dye molecules resulting from photoexcitation get reduced by receiving electrons from an electrolyte. The electrolyte is consequently regenerated through a neutraliza-

tion of the positive ions with the electrons coming from the counter electrode, which is a platinum film coated on a glass substrate connected to the external circuit. In such a photoelectrochemical system, the dye molecules are designed to be highly sensitive to visible light so they are able to play a role in catching the incident photons effectively.^{3,4} A variety of dyes have been intensively studied over the past two decades with attention being paid to increasing the molar extinction

Department of Materials Science and Engineering, University of Washington, Seattle WA, 98195, USA. E-mail: qfzhang@u.washington.edu; gzcao@u.washington.edu



Qifeng Zhang

Qifeng Zhang, Ph.D., is currently working at the University of Washington as a Research Assistant Professor. His research interests involve engineering applications of nano-structured materials on electrical devices including solar cells, UV light-emitting diodes (LEDs), field-effect transistors (FETs), and gas sensors. His current research focuses on the synthesis of nanomaterials and the application of nanomaterials in electronic and optoelectronic

devices, such as dye-sensitized solar cells (DSCs) and organic/inorganic hybrid solar cells.



Guozhong Cao

Guozhong Cao, Ph.D., is the Boeing-Steiner Professor of Materials Science and Engineering and Adjunct Professor of Chemical and Mechanical Engineering at the University of Washington. He has published over 250 refereed papers, and authored and edited 5 books, including "Nanostructures and Nanomaterials". His current research is focused mainly on nanomaterials for energy conversion and storage including solar cells, lithium-ion batteries, supercapacitors, and hydrogen storage materials.

coefficient and/or extending the absorption range into the longer wavelength area.⁵ Ruthenium complexes especially receive the most success in this regard and have become commercially available, known as N3, N719, and 'black dye', etc.⁶ On the other hand, the porous oxide film that acts as the *backbone* of the photoanode to carry the dye molecules has always been another one of the top concerns in the field of DSCs. At this point, the flourishing development of nanotechnology opens a door to tailoring the materials with various nanostructures. When used in DSCs, these nanostructures may provide a large surface area for dye adsorption and, moreover, make a difference to the behaviors of solar cells through affecting factors, such as the light propagation, electron transport, electrolyte (or I_3^- ions in electrolyte) diffusion within the photoelectrode film and so on. Recently developed hierarchically structured photoelectrodes are a good example of employing nanostructures to manage the light propagation and/or enhance the electron transport or ion diffusion in DSCs.

Hierarchically structured photoelectrodes are defined as a class of photoelectrodes that are made of films consisting of primary oxide nanostructures, for example, ZnO or TiO_2 nanocrystallites. However, these primary nanostructures form a secondary structure that is spherical or one-dimensional in shape. When used in DSCs, the hierarchically structured photoelectrode films not only provide a high surface area for the adsorption of dye molecules due to them consisting of nanomaterials, but also are able to offer extra functions to improve the solar cell performance by, for example, generating light scattering, enhancing the transport of injected electrons, and/or facilitating the diffusion of the electrolyte.

The advent of hierarchically structured photoelectrodes arises, to some extent, from the fact that the generation of light scattering in conventional DSCs with photoelectrodes made of nanocrystalline film relies on an additional topping layer that consists of large particles with a diameter of ~ 400 nm.⁷ Such a configuration, however, brings about an increase in the thickness of the photoelectrode film. As a result, those photogenerated

electrons at the light scattering layer would have to be transported a long distance within the photoelectrode film to reach the collective electrode and therefore suffer a high rate of recombination. Another problem comes from the low surface area of the large particles, which leads to a low amount of adsorption of the dye molecules and thus gives a limited gain in optical absorption.⁸ Besides these, the use of a topping layer for light scattering is also thought to be a non-optimal structure, in the respect that such a topping layer may hinder the diffusion of the electrolyte to some degree. Aside from the deficiencies of the double-layer structure, a photoelectrode comprised of nanocrystalline film alone is also problematic with the existence of numerous boundaries among the nanoparticles. These boundaries unavoidably lead to appreciable electron trapping and, thus, increase the rate of charge recombination that occurs at the nanoparticle/electrolyte interface, resulting from a reaction between the injected electrons and the positive species in the electrolyte.⁹ Such a recombination mechanism impairs the solar cell's performance by lowering both the open circuit voltage and the forward photocurrent. In addition to the drawback in electron transport, the nanocrystalline film is also thought to be disadvantageous in terms of pore size distribution, which is typically centered at an order of nanometres and is somewhat too small to allow for a quick diffusion of the electrolyte in the case of a DSC under operating conditions.

Generally, among all the hierarchical nanostructures, the spherical assemblies of ZnO or TiO_2 nanocrystallites have been most intensively studied for serving as photoelectrodes in DSCs during recent years.^{10–13} These assemblies possess a porous structure and therefore may ensure a large surface area for the adsorption of dye molecules. Meanwhile, due to their spherically shaped architecture with a diameter on the submicron meter scale, comparable to the wavelengths of visible light, these assemblies can generate effective light scattering in the sunlight spectrum. Another merit of the assemblies is that they can bring about a dense packing of nanocrystallites and, thus, facilitate the electron transport throughout the oxide film. In addition, it has also been

demonstrated that these spherical assemblies may form large pores in the photoelectrode film. This leads to a relatively open structure, which is believed to be beneficial for the diffusion of the electrolyte.

Besides the spherical assemblies, *quasi*-one-dimensional assemblies of nanocrystallites are also a kind of representative hierarchical structure that have been developed recently. Unlike spherical assemblies that put stress on light scattering, the *quasi*-one-dimensional assemblies of nanocrystallites emphasize direct pathways for electron transport that extend the electron diffusion length in DSCs.¹⁴

Spherical assemblies of nanocrystallites

ZnO aggregates

ZnO aggregates were developed and used in DSCs to form a hierarchical photoelectrode for the first time, being intended to offer a large surface area and light scattering ability simultaneously.^{10,15–17} The synthesis of ZnO aggregates was achieved by hydrolysis of zinc salt in a polyol medium at an elevated temperature (160 °C).^{10,18} The resultant aggregates are spherical in shape with diameters ranging from several tens to several hundred nanometres, consisting of ~ 15 nm ZnO nanocrystallites, and possessing a BET surface area of 80 ± 2 m² g⁻¹ (Figs 1a and b). The use of ZnO aggregates in DSCs as photoelectrode films demonstrated an efficiency of 5.4%, which was dramatically higher than the 2.4% obtained for the ZnO nanocrystallites (Fig. 1c). Such an enhancement in the conversion efficiency was attributed to light scattering generated by the aggregates due to their sizes, which are comparable to visible wavelengths. The existence of light scattering was explained to make a contribution to the photoelectrode by significantly extending the travelling distance of the light within the photoelectrode film and thus intensively increasing the probability of the incident photons interacting with the dye molecules. This finally resulted in an enhancement in the light harvesting efficiency of the photoelectrode as well as an improvement in the solar cell's performance.

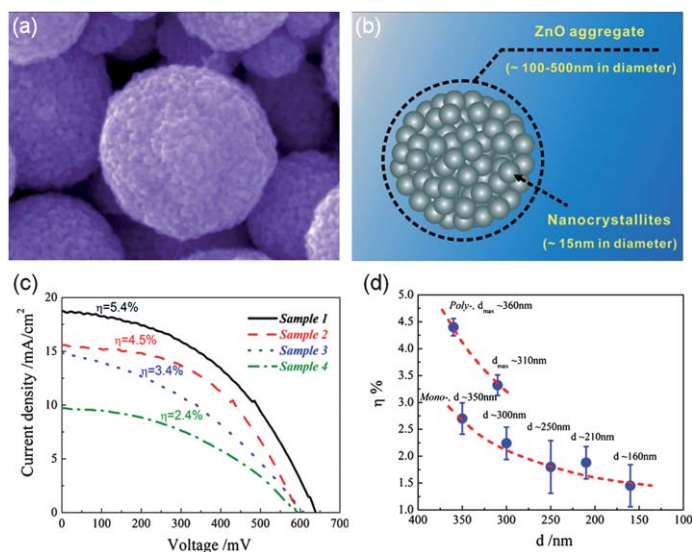


Fig. 1 The ZnO aggregates and their DSC performance. (a) A SEM image and (b) a schematic drawing of the ZnO aggregates consisting of nanocrystallites, (c) a comparison of solar cell efficiencies as the aggregates gradually lose their spherical morphology (Sample 1 and Sample 4 correspond to perfect aggregates and nanoparticles, respectively), and (d) the dependence of the solar cell efficiency on the aggregate size and size distribution.^{10,15}

The effect of light scattering was demonstrated by an experiment in which the spherical morphology of the ZnO aggregates was destroyed through raising the reaction temperature during their synthesis.¹⁰ The results revealed that the solar cell efficiency decreased as the aggregates gradually lost their spherical morphology (Fig. 1c). Such a structural evolution from the ideal aggregates to partially destroyed aggregates, or even dispersed nanoparticles, meant a gradual decrease in the light scattering. It was rational that the dispersed nanoparticles showed the lowest efficiency due to an absence of light scattering because the particle size was far smaller than the wavelengths of the incident light. The light scattering effect was further evidenced by another experiment demonstrating that the aggregates with a polydisperse size distribution might yield a higher conversion efficiency than those with a monodisperse size distribution (Fig. 1d). Moreover, in the case of the polydisperse aggregates, a broader size distribution had shown to result in better solar cell performance. This was explained by the fact that the aggregates with polydispersion and a broader size distribution might cause light scattering in a wider spectral range.¹⁵

It was also found that post-treatment of the photoelectrode film might also make

different impacts on the solar cell's performance depending on the annealing atmosphere, sintering temperature, and dye sensitization time. In one study in the literature, the photoelectrode film annealed in oxygen shows an efficiency approximately 50% higher than that obtained for the film annealed in air.¹⁹ On one hand, this might be explained by annealing in an oxygen atmosphere being helpful to reducing the surface defects of the ZnO nanocrystallites and thus suppresses the interfacial recombination of photo-generated electrons with a positive species in the electrolyte. On the other hand, annealing in oxygen could lower the oxygen vacancy defects of the ZnO nanocrystallites and accordingly reduce the trapping of electrons during transport. The impact of the sintering temperature on the solar cell's performance likely originates from a shrinkage of the aggregates while the sintering temperature is above 350 °C, which results in an appreciable decrease in the surface area of the photoelectrode film.²⁰ The sensitization time in the dye solution is another critical factor that should be paid particular attention to in the case of ZnO materials. A sensitization time longer than, for example, 30 min may lead to the formation of a Zn²⁺/dye complex, which is inactive to electron injection and can do harm to the solar cell's efficiency instead of improving it.²¹

ZnO hollow spheres

ZnO hollow spheres are a structure similar to the ZnO aggregates mentioned above, however, the assemblies of nanocrystallites form a shell structure with a hollow interior. The synthesis of ZnO hollow spheres was reported to be a sonochemical process, which involves ultrasonication treatment of a solution containing zinc acetate, dimethyl sulfoxide (DMSO) and water.²² The use of ZnO hollow spheres in DSCs has demonstrated an efficiency of 4.33%. Such a value is approximately 20% lower than the 5.4% obtained for the ZnO aggregates, probably due to the insufficiency in the internal surface area in view of the hollow structure. However, compared to the ZnO nanoparticles, the ZnO hollow spheres still presented a higher conversion efficiency (4.33% for ZnO hollow spheres, and 3.12% for ZnO nanoparticles) in spite of a lower amount of dye adsorption ($6.81 \times 10^{-8} \text{ mol cm}^{-2}$ for the ZnO hollow spheres, $9.78 \times 10^{-8} \text{ mol cm}^{-2}$ for the ZnO nanoparticles). Such a scenario well evidences that the light scattering effect arising from the hollow spheres plays a significant role in increasing the optical absorption of the photoelectrode.

Mesoporous TiO₂ beads

Mesoporous TiO₂ beads were prepared through solvothermal treatment of amorphous precursor TiO₂ spheres. These are a kind of spherical assembly of TiO₂ nanocrystallites, exhibiting a structure similar to the ZnO aggregates (Figs 2a through d).^{11,12,23,24} These mesoporous beads typically feature a diameter of 830 ± 40 nm, a nanocrystallite diameter size of 12.2 ± 0.3 nm, and a BET surface area of 108.0 m² g⁻¹. It was also demonstrated that the pore size of the beads could be adjusted in the range 14–23 nm by changing the concentration of ammonia employed in the solution during solvothermal treatment.²³ A comparison of the dye adsorption capability of the mesoporous TiO₂ beads and P25 nanocrystals (a kind of commercial powder of TiO₂ nanoparticles with an average diameter of 20 nm, Degussa, Germany) revealed saturation adsorption capabilities of 8.69 × 10⁻⁵ mol g⁻¹ and 4.25 × 10⁻⁵ mol g⁻¹ for the mesoporous

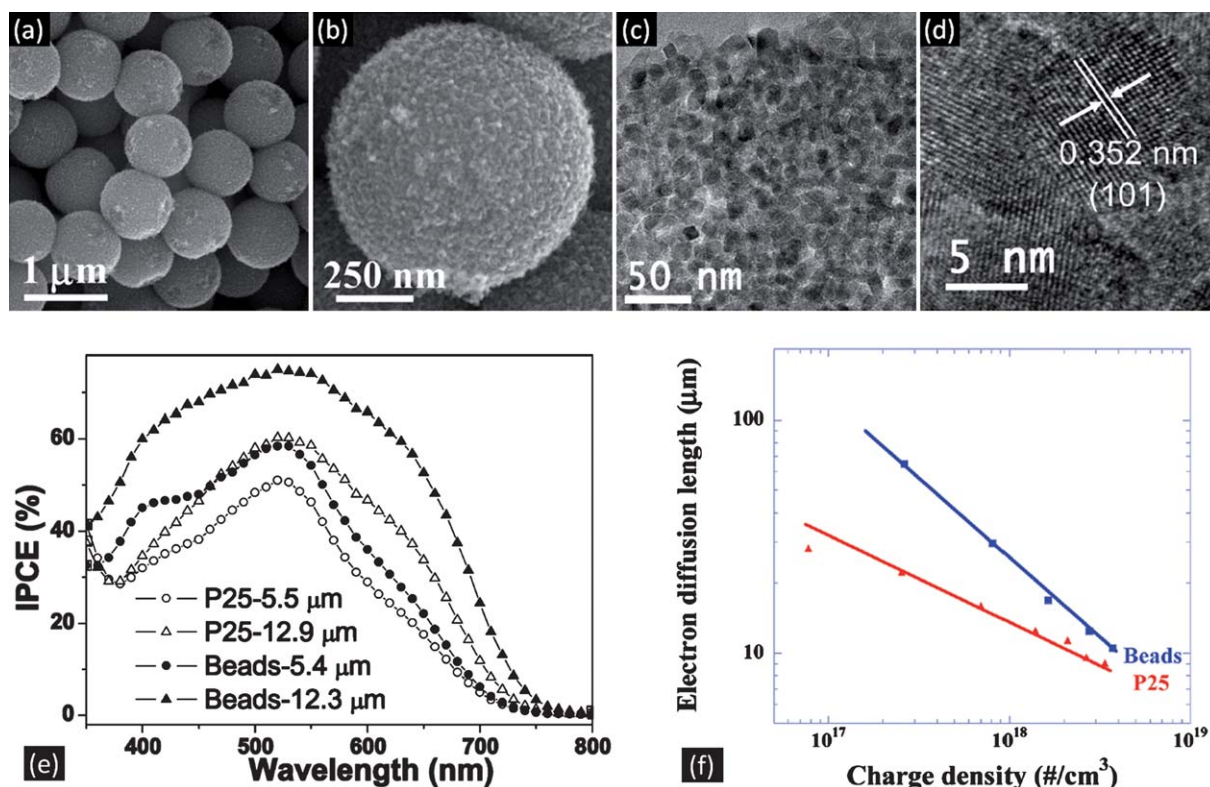


Fig. 2 The morphology, structure and DSC performance of the mesoporous TiO₂ beads. (a), (b) SEM images and (c), (d) TEM images of the mesoporous TiO₂ beads, (e) IPCE spectra and (f) a comparison of the electron diffusion length in DSCs made of mesoporous TiO₂ beads or P25 nanoparticles.^{11,12,23}

TiO₂ beads and P25 nanocrystals, respectively. This result strongly suggests that (1) the internal surface of the mesoporous TiO₂ beads can be readily accessed by the dye molecules, and (2) while forming a photoelectrode film, the mesoporous beads may provide a higher internal surface area than the dispersed nanocrystallites due to the compact packing inside the beads. Such structural features of the mesoporous TiO₂ beads contribute to the solar cell, as shown on the incident photon to current conversion efficiency (IPCE) spectra that exhibit an efficiency enhancement due to a higher dye adsorption capability compared to the dispersed nanocrystals (P25) in the visible region (370–600 nm) and a light scattering effect in the near-infrared region (600–750 nm, where the organic dye has a very low absorption) (Fig. 2e). As a result, the mesoporous TiO₂ beads presented an efficiency of 7.20%, which was 27% higher than the 5.66% obtained for the dispersed nanocrystals.

Aside from a large internal surface area and light scattering capability, the mesoporous TiO₂ beads have also been indi-

cated to give a longer electron diffusion length (L_n) than in the case of dispersed nanocrystals (Fig. 2f).¹² This was attributed to the well interconnected network of the nanocrystallites within the mesoporous beads, leading to an improvement in electron transport and therefore a decrease in the interfacial charge recombination rate.

Nanoporous TiO₂ spheres

Rather than emphasizing the light scattering effect or the compact interconnection of nanocrystallites within the assemblies, another investigation carried out on nanoporous TiO₂ spheres argues that the enhancement of solar cell performance is primarily due to the open structure of the photoelectrode film in the respect that the film is constructed with submicron-sized nanoporous spheres.¹³ Through using the electrical impedance spectroscopy (EIS) technique to compare solar cells constructed with TiO₂ spheres with the ideal spherical morphology (DSC-1, Fig. 3a), spheres with a slightly deformed spherical morphology (DSC-2,

Fig. 3b) and the dispersed nanoparticles (DSC-3), it was found that (1) the response in the high-frequency region, which represented the interfacial resistance between the fluorine-doped tin oxide (FTO) and the TiO₂ layer, revealed that the deformed spheres (DSC-2) presented a resistance smaller than that of the perfect spheres (DSC-1) and similar to that of the nanoparticles (DSC-3), indicating good contact between the deformed spheres and the FTO film, and (2) the diffusion constants of the I₃⁻ ions in the electrolyte, represented by the response in the low-frequency region, were 6.7×10^{-6} , 4.9×10^{-6} , and 4.1×10^{-6} for DSC-1, DSC-2, and DSC-3, respectively. This suggested that the spheres could form large external pores (denoted “A” in Fig. 3c) and thus provide a “highway” for the electrolyte diffusion throughout TiO₂ layer; quick diffusion of the electrolyte in the film enables the I₃⁻ ions to further diffuse into the internal pores (denoted “B”) more efficiently, owing to a short diffusion distance from the outside to the interior of the spheres (Fig. 3c).

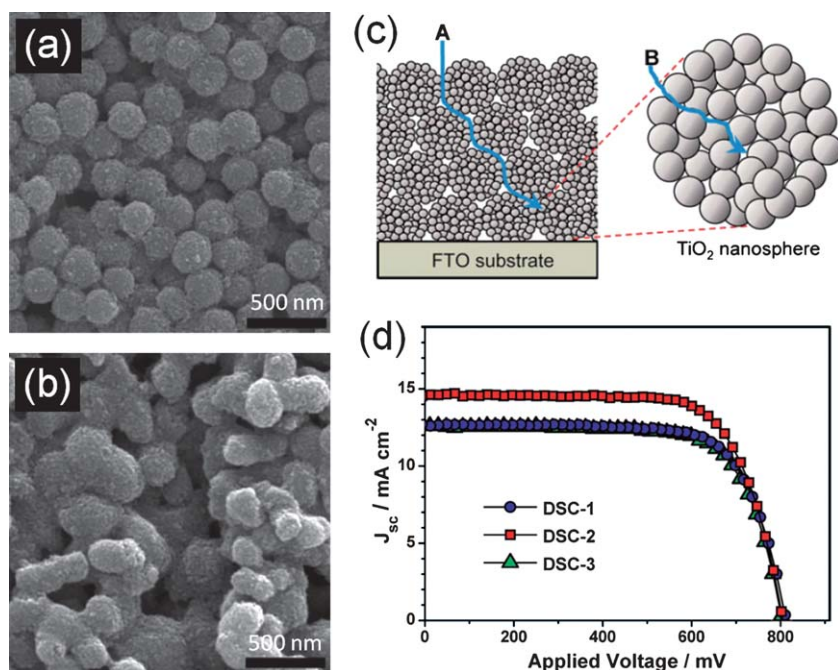


Fig. 3 Nanoporous TiO₂ spheres presenting good DSC performance by improving electrolyte diffusion. (a) and (b) SEM images of perfect spheres and deformed spheres, respectively, (c) a schematic of electrolyte diffusion through large external pores (denoted as “A”) and small internal pores (denoted as “B”), and (d) a comparison of solar cell performance of perfect spheres (DSC-1), deformed spheres (DSC-2), and commercial nanoparticles (DSC-3).¹³

The attainment of deformed spheres was described to be a result of precursor solution containing starting materials (titanium isopropoxide, TTIP) in higher concentration than that for the synthesis of perfect spheres *via* a two step method.¹³ Typical nanoporous TiO₂ spheres possess a size of ~250 nm in diameter and consist of 12–13-nm-sized TiO₂ grains (Fig. 3a and b). The efficiencies of solar cells made of nanoporous spheres are 8.44% and 7.43% for deformed spheres and perfect spheres, respectively, which are generally higher than the 7.30% obtained for commercial nanoparticles (DyeSol Co.) (Fig. 3d). The merit of deformed spheres

was explained to be that, compared to perfect spheres, they had smaller internal pore size and their irregular shape might give rise to better contact between the TiO₂ layer and the FTO film as well as better connection between the neighboring spheres.

Quasi-one-dimensional assemblies of nanocrystallites

TiO₂ forest

A TiO₂ forest is a hierarchically structured film comprised of *quasi*-one-dimensional assemblies of nano-

crystallites, morphologically showing a forest-like architecture. The creation of the TiO₂ forest was based on a pulsed laser deposition (PLD) process, through which an amorphous film was fabricated on a TiO₂-coated FTO glass substrate by ablation of a Ti target in an O₂ atmosphere.¹⁴ Annealing in air at 500 °C was then performed to obtain the anatase crystalline phase.²⁵ The film architecture was found to be dependent on the oxygen pressure during film deposition. Only in a narrow window of operating conditions, with an oxygen pressure between 10 and 100 Pa, could the forest-like morphology be attained. The oxygen pressure might also affect the surface area and porosity of the resultant film, for example, yielding a surface area of 37 m² g⁻¹ and a porosity of 68% at 20 Pa, and 86 m² g⁻¹ and 79% at 40 Pa. A typical TiO₂ forest is constructed with one-dimensional assemblies, which consist of 10 nm nanocrystallites that form “trees” with a height in the micrometre scale and branches in the 100 nm scale (Fig. 4a). The film thickness, *i.e.*, the height of the “trees”, increased linearly with the deposition time and deposition rate (up to 1 μm min⁻¹, depending on the experimental conditions).

The characteristics of the TiO₂ forest, *i.e.*, *quasi*-one-dimensional assemblies of nanocrystallites, enable such kinds of film to be large in surface area and have a one-dimensional structure that may provide direct pathways for electron transport and, thus, lower the interfacial charge recombination.²⁶ This point was manifested by a comparison between the TiO₂ tree films and the nanocrystalline films in terms of the electron lifetime using the EIS technique. The results revealed that the TiO₂ tree films exhibited a significantly longer electron lifetime (τ_n), by more than 1 order of magnitude, in comparison to the TiO₂ nanocrystalline films (Fig. 4b). Such an improvement in the electron lifetime was attributed to the possibility that the one-dimensional structure of the TiO₂ forest film might be beneficial to charge collection as similarly experienced on films composed of perpendicular arrays of ZnO nanowires^{26,27} or TiO₂ nanotubes.^{28–30}

Conclusions and outlook

Hierarchically structured photoelectrodes were highlighted with regard to their

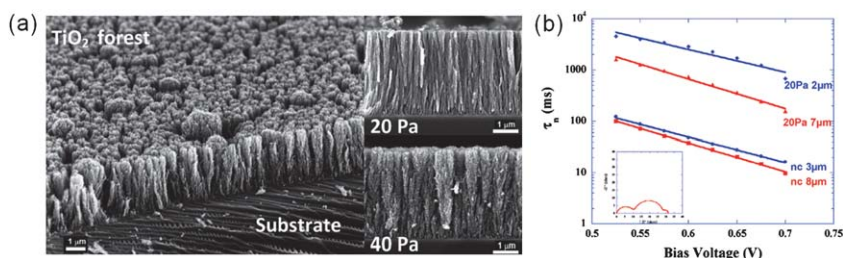


Fig. 4 A TiO₂ forest-like structure presenting an improvement in the electron lifetime compared to nanocrystallites when used in DSCs. (a) SEM images of TiO₂ forest films, the insets show the different structures of the films PLD-produced under different oxygen pressures, and (b) the evolution of the lifetime as a function of bias voltage for the TiO₂ forest films and the nanocrystalline films.¹⁴

capability of enhancing DSC performance. The main structural feature of the hierarchical photoelectrodes is that the photoelectrode film is constructed with spherical or one-dimensional assemblies of nanocrystallites, which form a class of nanostructures appearing in the literature as so-called *ZnO aggregates*, *ZnO hollow spheres*, *mesoporous TiO₂ beads*, *nanoporous TiO₂ spheres*, and *TiO₂ forests*. These nanostructures not only provide a large surface area, when used for DSCs, but also present extra functions, such as (1) generating light scattering, (2) strengthening electron transport, and/or (3) facilitating electrolyte diffusion. Solar cells benefit from these extra functions due to an enhancement in light harvesting efficiency, charge collection efficiency of the photoelectrode, and/or internal circulation efficiency of the cell.

This paper ends with an emphasis on the light scattering effect of hierarchical photoelectrodes. This is based on considerations that the existence of light scattering would allow the photoelectrode to be constructed with a single layer film rather than a double-layer configuration, which is a method usually employed in the conventional DSCs, however this makes the fabrication process more complex and potentially increases the cost of manufacture. Moreover, due to the light scattering that may improve the light harvesting efficiency of photoelectrode films, it therefore becomes potentially possible for these hierarchical films to have a thickness smaller than that of the traditional ones without showing a diminution in the light absorption. Allowing for thinner photoelectrode films is important, since it means a shortening of the distance for the photogenerated electrons to travel from the site of electron injection to the FTO film of the collecting electrode. As such, the charge recombination rate can be significantly lowered and therefore, one can expect a breakthrough in the dye-sensitized solar cell efficiency, which is ~11% at present.

Undeniably, for the photoelectrodes comprised of spherically structured aggregates, there exists a disadvantage in the transport of the injected electrons

through the neighboring aggregates due to the relatively small contact area among the aggregates. Such a problem can be solved to some extent by employing deformed spherical aggregates, as described by Kim *et al.*,¹³ to improve the connection between the neighboring aggregates. Another possible way of compensating the small contact area is to adopt a mixed structure comprised of aggregates and nanoparticles, in which the nanoparticles would fill up the voids among the aggregates and thus play a role in bridging the aggregates, so as to enhance the transport of the photo-generated electrons within the photoelectrode film.

Acknowledgements

This work is supported by the U.S. Department of Energy, Office of Basic Energy Sciences, Division of Materials and Engineering under Award No. DE-FG02-07ER46467 (Q.F.Z.), National Science Foundation (DMR 1035196), the Air Force Office of Scientific Research (AFOSR-MURI, FA9550-06-1-0326) (K. S.P.), the University of Washington TGIF grant, the Washington Research Foundation and the Intel Corporation.

References

- 1 M. Gratzel, *Nature*, 2001, **414**, 338–344.
- 2 M. Gratzel, *Inorg. Chem.*, 2005, **44**, 6841–6851.
- 3 A. Polo, M. Itokazu and N. Murakami Iha, *Coord. Chem. Rev.*, 2004, **248**, 1343–1361.
- 4 M. Nazeeruddin, C. Klein, P. Liska and M. Grätzel, *Coord. Chem. Rev.*, 2005, **249**, 1460–1467.
- 5 A. S. Polo, M. K. Itokazu and N. Y. Murakami Iha, *Coord. Chem. Rev.*, 2004, **248**, 1343–1361.
- 6 J. Kroon, N. Bakker, H. Smit, P. Liska, K. Thampi, P. Wang, S. Zakeeruddin, M. Grätzel, A. Hinsch and S. Hore, *Progr. Photovolt.: Res. Appl.*, 2007, **15**, 1–18.
- 7 S. Ito, T. Murakami, P. Comte, P. Liska, C. Grätzel, M. Nazeeruddin and M. Grätzel, *Thin Solid Films*, 2008, **516**, 4613–4619.
- 8 H. J. Koo, Y. J. Kim, Y. H. Lee, W. I. Lee, K. Kim and N. G. Park, *Adv. Mater.*, 2008, **20**, 195–199.
- 9 A. J. Frank, N. Kopidakis and J. van de Lagemaat, *Coord. Chem. Rev.*, 2004, **248**, 1165–1179.
- 10 Q. F. Zhang, T. R. Chou, B. Russo, S. A. Jenekhe and G. Z. Cao, *Angew. Chem., Int. Ed.*, 2008, **47**, 2402–2406.
- 11 D. H. Chen, F. Z. Huang, Y. B. Cheng and R. A. Caruso, *Adv. Mater.*, 2009, **21**, 2206–2210.
- 12 F. Sauvage, D. H. Chen, P. Comte, F. Z. Huang, L. P. Heiniger, Y. B. Cheng, R. A. Caruso and M. Graetzel, *ACS Nano*, 2010, **4**, 4420–4425.
- 13 Y. J. Kim, M. H. Lee, H. J. Kim, G. Lim, Y. S. Choi, N. G. Park, K. Kim and W. I. Lee, *Adv. Mater.*, 2009, **21**, 3668–3673.
- 14 F. Sauvage, F. Di Fonzo, A. L. Bassi, C. S. Casari, V. Russo, G. Divitini, C. Ducati, C. E. Bottani, P. Comte and M. Graetzel, *Nano Lett.*, 2010, **10**, 2562–2567.
- 15 Q. F. Zhang, T. P. Chou, B. Russo, S. A. Jenekhe and G. Cao, *Adv. Funct. Mater.*, 2008, **18**, 1654–1660.
- 16 T. P. Chou, Q. F. Zhang, G. E. Fryxell and G. Z. Cao, *Adv. Mater.*, 2007, **19**, 2588–2592.
- 17 Q. F. Zhang, C. S. Dandeneau, X. Y. Zhou and G. Z. Cao, *Adv. Mater.*, 2009, **21**, 4087–4108.
- 18 D. Jezequel, J. Guenot, N. Jouini and F. Fievet, *J. Mater. Res.*, 1995, **10**, 77–83.
- 19 Y. Z. Zhang, L. H. Wu, Y. P. Liu and E. Q. Xie, *J. Phys. D: Appl. Phys.*, 2009, **42**, 085105.
- 20 Q. F. Zhang, T. P. Chou, B. Russo, S. A. Jenekhe and G. Cao, *Adv. Funct. Mater.*, 2008, **18**, 1654–1660.
- 21 T. P. Chou, Q. F. Zhang and G. Z. Cao, *J. Phys. Chem. C*, 2007, **111**, 18804–18811.
- 22 C. X. He, B. X. Lei, Y. F. Wang, C. Y. Su, Y. P. Fang and D. B. Kuang, *Chem.-Eur. J.*, 2010, **16**, 8757–8761.
- 23 D. H. Chen, L. Cao, F. Z. Huang, P. Imperia, Y. B. Cheng and R. A. Caruso, *J. Am. Chem. Soc.*, 2010, **132**, 4438–4444.
- 24 F. Z. Huang, D. H. Chen, X. L. Zhang, R. A. Caruso and Y. B. Cheng, *Adv. Funct. Mater.*, 2010, **20**, 1301–1305.
- 25 F. Di Fonzo, C. S. Casari, V. Russo, M. F. Brunella, A. L. Bassi and C. E. Bottani, *Nanotechnology*, 2009, **20**, 015604.
- 26 M. Law, L. E. Greene, J. C. Johnson, R. Saykally and P. D. Yang, *Nat. Mater.*, 2005, **4**, 455–459.
- 27 E. Galoppini, J. Rochford, H. Chen, G. Saraf, Y. Lu, A. Hagfeldt and G. Boschloo, *J. Phys. Chem. B*, 2006, **110**, 16159–16161.
- 28 G. K. Mor, O. K. Varghese, M. Paulose, K. Shankar and C. A. Grimes, *Sol. Energy Mater. Sol. Cells*, 2006, **90**, 2011–2075.
- 29 G. Mor, K. Shankar, M. Paulose, O. Varghese and C. Grimes, *Nano Lett.*, 2006, **6**, 215–218.
- 30 C. Grimes, *J. Mater. Chem.*, 2007, **17**, 1451–1457.